

# Sub-50 fs Yb-doped laser with anomalous-dispersion photonic crystal fiber

Zuxing Zhang,<sup>1,\*</sup> Ç. Şenel,<sup>1,2</sup> R. Hamid,<sup>2</sup> and F. Ö. Ilday<sup>1</sup>

<sup>1</sup>Department of Physics, Bilkent University, Ankara 06800, Turkey

<sup>2</sup>TÜBİTAK National Metrology Institute (UME), Kocaeli 41470, Turkey

\*Corresponding author: zhang@fen.bilkent.edu.tr

Received January 8, 2013; revised February 12, 2013; accepted February 12, 2013;  
posted February 13, 2013 (Doc. ID 183054); published March 13, 2013

We report on the generation of 42 fs pulses at 1  $\mu\text{m}$  in a completely fiber-integrated format, which are, to the best of our knowledge, the shortest from all-fiber-integrated Yb-doped fiber lasers to date. The ring fiber cavity incorporates anomalous-dispersion, solid-core photonic crystal fiber with low birefringence, which acts as a broadband, in-fiber Lyot filter to facilitate mode locking. The oscillator operates in the stretched-pulse regime under slight normal net cavity dispersion. The cavity generates 4.7 ps long pulses with a spectral bandwidth of 58.2 nm, which are dechirped to 42 fs via a grating pair compressor outside of the cavity. Relative intensity noise (RIN) of the laser is characterized, with the integrated RIN found to be 0.026% in the 3 Hz–250 kHz frequency range. © 2013 Optical Society of America

OCIS codes: 060.2320, 140.7090, 190.4370, 320.7090.

An intense research effort has been channeled into improving understanding and technical performance of mode-locked fiber laser oscillators in recent years. These efforts have led to the discovery of new mode-locking regimes [1–3] and new theoretical treatments [4,5], increased pulse energies [6,7], decreased pulse durations [8], unearthed rich dynamical behavior [9,10], and demonstrated excellent frequency comb performance [11]. Dispersion management is often employed to reach pulse durations below 50 fs, which is implemented most commonly with bulk optical components, such as diffraction gratings, in Yb-doped fiber lasers [12]. Increased robustness against environmental perturbations remains a valuable trait, for which all-fiber integration is highly desirable. Several techniques for fiber-based anomalous dispersion have been utilized, such as tapered fibers [13], chirped fiber Bragg gratings [14], photonic crystal fibers (PCFs) [15] and hollow-core photonic bandgap fibers [16,17]. Fabrication of sufficiently long fiber tapers demands great precision; chirped fiber Bragg gratings have limited bandwidth, and hollow-core photonic bandgap fibers suffer from poor matching with standard fibers. Solid-core PCFs have small mode field diameters, enhancing nonlinear effects, and usually are birefringent. The first mode-locked laser to incorporate a PCF was reported in 2002 by Lim *et al.* [15]. Indeed, mode locking was not self-starting, due to the residual birefringence of the PCF. Since then, a number of dispersion-managed Yb-doped fiber lasers using PCFs and all-fiber-integrated lasers have been reported. After 10 years, no all-fiber-integrated Yb-fiber laser has been demonstrated to support pulses below 60 fs [18].

Here, we present an all-fiber-integrated, dispersion-managed Yb-doped oscillator incorporating a segment of PCF. The oscillator is self-starting and generates pulses with a spectral bandwidth of 58.2 nm, compressible externally to 42 fs. The pulse evolution and the cavity layout had to be carefully designed to achieve this performance: the residual birefringence that prevented self-starting operation of the first fiber laser with PCF [15] is actively employed to construct an intracavity Lyot

filter to ease initiation of mode locking [19]. The pulse energy is reduced to  $\sim 78$  pJ in the PCF to prevent excessive nonlinear effects. This requires an intracavity gain of 60 to reach the maximum pulse energy of 4.7 nJ, and self-similar evolution in part of the gain fiber is utilized to prevent gain narrowing.

The experimental setup is shown in Fig. 1. The gain section of the oscillator is 1.88 m long ytterbium-doped fiber (YDF), followed by a 10% output coupler and an in-line isolator. Up to 500 mW of pump light from a 976 nm pump diode is delivered via a 980/1060 nm wavelength-division multiplexer (WDM). The YDF has a group-velocity dispersion (GVD) of  $35.7$  fs<sup>2</sup>/mm at 1.05  $\mu\text{m}$ . A polarizer flanked by two polarization controllers (PCs) implements nonlinear polarization evolution. A section of solid-core PCF with a length of 2.1 m, directly spliced to single-mode fiber (SMF) with a modified electric arc fusion method, is utilized to manage the cavity

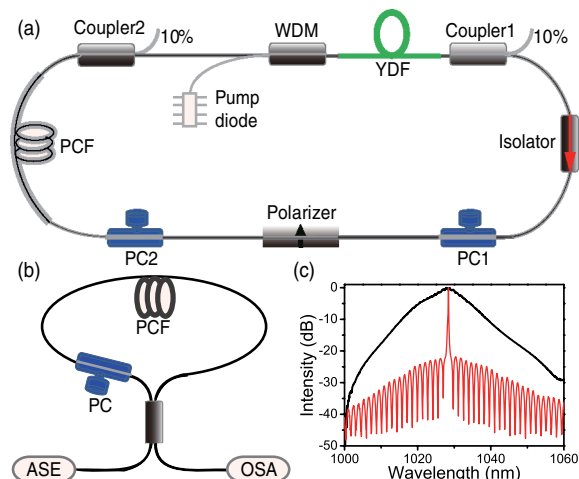


Fig. 1. (Color online) (a) Schematic of the all-fiber Yb-doped laser using PCF for dispersion compensation, (b) Sagnac loop constructed to measure the birefringence of the PCF, and (c) spectrum of the ASE signal entering the Sagnac loop (black, top curve) and the spectrum of the signal transmitted through the Sagnac loop (red curve). OSA, optical spectrum analyzer.

dispersion. The insertion loss is about 10 dB. The PCF has an air-hole spacing of  $2.0\ \mu\text{m}$  and an air-hole diameter of  $1.2\ \mu\text{m}$  (characterized using a scanning electron microscope), corresponding to an effective area of  $3.15\ \mu\text{m}^2$  and a nonlinear coefficient of  $52\ \text{W}^{-1}\text{km}^{-1}$ . The dispersion of the PCF was calculated to be  $-44.8\ \text{fs}^2/\text{mm}$  at  $1.05\ \mu\text{m}$  using numerical simulations of the wave propagation and a model of fiber created according to the measured parameters. The other fibers, including pig-tails of all components, are standard SMF with a GVD of  $20.7\ \text{fs}^2/\text{mm}$  and a total length of 1.68 m. It is optimal to keep the net dispersion of the cavity close to zero for minimum pulse duration [20]. Thus, we have set it to near-zero, at slightly normal dispersion, estimated to be  $0.008\ \text{ps}^2$ . This is necessary to support acceptable levels of pulse energy despite the exceptionally small mode area of the PCF.

We measured the birefringence of the PCF using a Sagnac loop, seeded by a homemade amplified spontaneous emission (ASE) source and consisting of a 50:50 coupler, a PC, and a 26 m long segment of the PCF [Fig. 1(b)]. The Sagnac output exhibited a comb-like spectrum with wavelength spacing of 2.4 nm. Given  $\Delta n = (\lambda^2)/(\Delta\lambda L)$ , we deduced that the birefringence of the PCF is  $2 \times 10^{-5}$  and calculated that the corresponding bandwidth of the Lyot filter is approximately 30 nm for the 2.1 m long PCF used in the mode-locked laser.

Numerical simulations based on the model described in [3] were performed to investigate the mode-locking dynamics (Fig. 2). The pulse duration and spectral bandwidth decrease in the first half of the gain fiber, then grow essentially self-similarly until the saturable absorber. Initial compression in the PCF is followed by stretching, accompanied by spectral broadening and narrowing. The output spectra, measured after the YDF and PCF, have bandwidths of 64 and 43 nm, respectively [Fig. 2(b)]. Figure 2(c) shows a 3.2 ps long pulse after the YDF with nearly parabolic shape. While the overall evolution is consistent with stretched-pulse operation

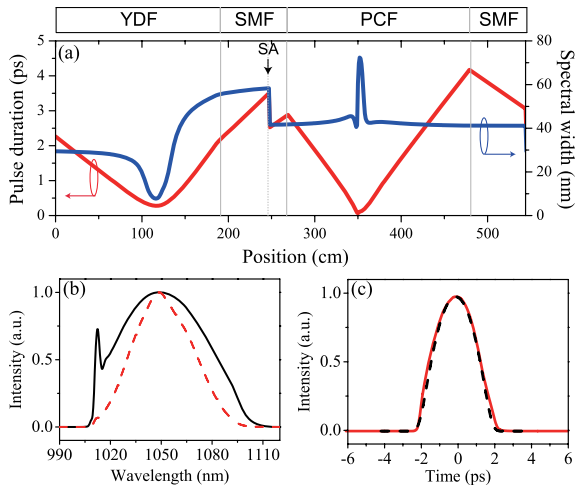


Fig. 2. (Color online) Simulated results. (a) Evolution of the spectral and temporal widths as a function of position along the cavity, (b) spectra after the YDF (solid curve) and after the PCF (dashed curve), and (c) pulse shape after the YDF (red, solid curve) and parabolic fit (black, dashed curve).

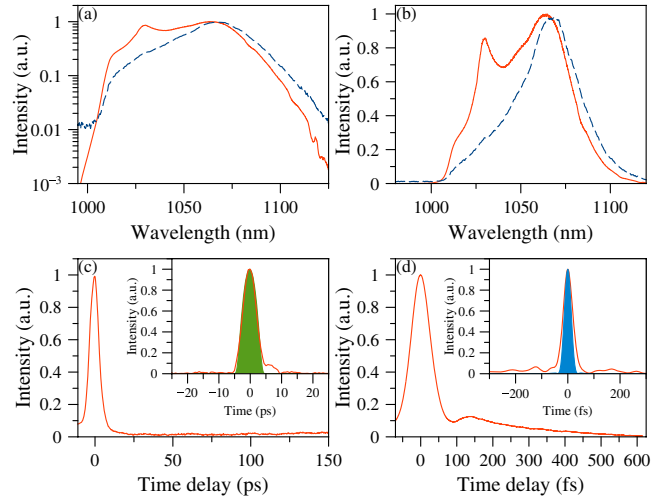


Fig. 3. (Color online) Optical spectra measured from couplers before (dashed curve) and after (solid curve) YDF on (a) a logarithmic scale and (b) a linear scale. (c) Autocorrelation trace of the chirped pulse. Inset shows retrieved chirped pulse shape (solid curve) and its parabolic fit (filled curve). (d) Autocorrelation trace of the dechirped pulse. Inset shows retrieved dechirped pulse shape (solid curve) and transform-limited pulse (filled curve).

[21], influence of self-similar evolution in the gain fiber is observed due to the strong nonlinearity, which was necessary to balance gain narrowing.

Due to the filtering effect of the PCF, self-starting mode locking with a repetition rate of 35.7 MHz was obtained at pump powers above 230 mW. The pulse spectra broadened from a full width at half-maximum (FWHM) of 42.6 nm (27.3 nm) at threshold power to over 58.2 nm (38.4 nm) at maximum available pump power after the gain fiber (PCF). This broadening should continue until either multiple pulses or CW breakthrough occurs, but neither of these effects occurred within the range of our available pump power. The spectra at maximum power are shown in Figs. 3(a) and 3(b). Average powers extracted from the couplers after the YDF and the PCF are 16.8 and 0.28 mW, corresponding to intracavity pulse energies of 4.7 nJ and 78 pJ, respectively. The width of the chirped pulse extracted from the coupler after the gain fiber was measured to be 4.7 ps [Fig. 3(c)]. The temporal profile of the chirped pulse was retrieved from the autocorrelation and spectrum data using the PICASO algorithm [22]. The shape is essentially parabolic, confirming the role of self-similar evolution in the latter part of the gain fiber [inset of Fig. 3(c)]. The pulses are compressed to an FWHM duration of 42 fs [Fig. 3(d)] by applying dispersion of  $-0.044\ \text{ps}^2$ , which is smaller than the anomalous dispersion induced by the PCF. This implies that the pulses circulating in the laser cavity are chirp-free at a point near the middle of the PCF, consistent with the numerical simulations and stretched pulse operation [21]. The PICASO-retrieved shape of the compressed pulse is shown in the inset of Fig. 3(d). The corresponding Fourier transform-limited pulse width is  $\sim 27\ \text{fs}$ . The deviation from the transform limit and the presence of a pedestal is attributed to the strong higher-order dispersion arising from the PCF.

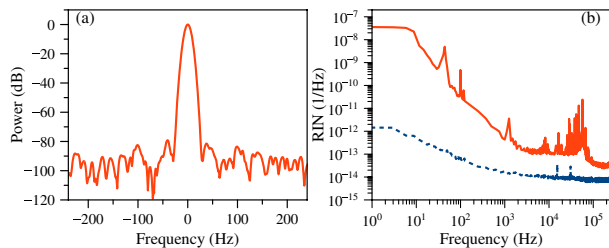


Fig. 4. (Color online) (a) Measured RF spectrum with 500 Hz span and 1 Hz resolution with central frequency shifted to zero for clarity and (b) measured RIN spectrum (solid curve) and measurement noise level (dotted curve).

The stability of the laser was investigated using an RF spectrum analyzer and a baseband spectrum analyzer. Figure 4(a) is a close-up RF spectrum of the fundamental repetition frequency, with a 1 Hz resolution bandwidth, showing 80 dB sideband suppression without averaging. Figure 4(b) shows the relative intensity noise (RIN) spectrum, the details of which can be found in [23]. The integrated RIN (over 3 Hz–250 kHz) is 0.026%. These results confirm that the laser has excellent pulse-to-pulse stability with no degradation compared to Yb-fiber lasers with bulk dispersion-compensating components.

In conclusion, we have demonstrated an all-fiber-integrated Yb-doped laser with an anomalous-dispersion PCF. The spectral width of the pulses is 58 nm, and the compressed pulse duration is 42 fs, which is the shortest, to the best of our knowledge, from an all-fiber oscillator at 1  $\mu\text{m}$ . Mode-locked operation is self-starting and long-term stable. These results have been achieved 10 years after the first mode-locked oscillator with PCF was demonstrated, which was plagued with nonself-starting operation and limited long-term stability primarily due to the residual birefringence of the PCF. Here, the birefringence of the PCF is exploited to function as a fiber-integrated Lyot filter of suitable bandwidth for stable and self-starting mode locking. Nonlinear spectral shaping throughout the cavity and self-similar evolution in the second half of the gain fiber are carefully managed to avoid multiple pulsing, while retaining a large bandwidth and low-noise operation, despite amplification by a factor of 60.

This work was supported by TÜBİTAK under grant nos. 209T058 and 109T350 and the European Union (EU) FP7 CROSS-TRAP Project (grant no. 244068).

## References

1. F. Ö. Ilday, J. R. Buckley, W. G. Clark, and F. W. Wise, *Phys. Rev. Lett.* **92**, 213902 (2004).
2. A. Chong, J. Buckley, W. Renninger, and F. W. Wise, *Opt. Express* **14**, 10095 (2006).
3. B. Oktem, C. Ülgüdür, and F. Ö. Ilday, *Nat. Photonics* **4**, 307 (2010).
4. C. R. Jones and J. N. Kutz, *J. Opt. Soc. Am. B* **27**, 1184 (2010).
5. C. Jirauschek and F. Ö. Ilday, *Phys. Rev. A* **83**, 063809 (2011).
6. J. R. Buckley, F. Ö. Ilday, and F. W. Wise, *Opt. Lett.* **30**, 1888 (2005).
7. F. Röser, T. Eidam, J. Rothhardt, O. Schmidt, D. N. Schimpf, J. Limpert, and A. Tünnermann, *Opt. Lett.* **32**, 3495 (2007).
8. A. Chong, H. Liu, B. Nie, B. G. Bale, S. Wabnitz, W. H. Renninger, M. Dantus, and F. W. Wise, *Opt. Express* **20**, 14213 (2012).
9. S. Chouli and P. Grelu, *Opt. Express* **17**, 11776 (2009).
10. B. Ortac, A. Hideur, M. Brunel, C. Chedot, J. Limpert, A. Tünnermann, and F. Ö. Ilday, *Opt. Express* **14**, 6075 (2006).
11. T. R. Schibli, I. Hartl, D. C. Yost, M. J. Martin, A. Marcinkevičius, M. E. Fermann, and J. Ye, *Nat. Photonics* **2**, 355 (2008).
12. H. Lim, F. Ö. Ilday, and F. W. Wise, *Opt. Lett.* **28**, 660 (2003).
13. M. Rusu, R. Herda, S. Kivistö, and O. G. Okhotnikov, *Opt. Lett.* **31**, 2257 (2006).
14. S. Kivistö, R. Herda, and O. G. Okhotnikov, *Opt. Express* **16**, 265 (2008).
15. H. Lim, F. Ö. Ilday, and F. W. Wise, *Opt. Express* **10**, 1497 (2002).
16. H. Lim, A. Chong, and F. W. Wise, *Opt. Express* **13**, 3460 (2005).
17. A. Ruehl, O. Prochnow, M. Engelbrecht, D. Wandt, and D. Kracht, *Opt. Lett.* **32**, 1084 (2007).
18. M. Schultz, O. Prochnow, A. Ruehl, D. Wandt, D. Kracht, S. Ramachandran, and S. Ghalmi, *Opt. Lett.* **32**, 2372 (2007).
19. K. Özgören and F. Ö. Ilday, *Opt. Lett.* **35**, 1296 (2010).
20. F. Ö. Ilday, J. Buckley, L. Kuznetsova, and F. W. Wise, *Opt. Express* **11**, 3550 (2003).
21. K. Tamura, E. P. Ippen, and H. A. Haus, *Appl. Phys. Lett.* **67**, 158 (1995).
22. J. W. Nicholson, J. Jasapara, W. Rudolph, F. G. Omenetto, and A. J. Taylor, *Opt. Lett.* **24**, 1774 (1999).
23. I. L. Budunoglu, C. Ülgüdür, B. Oktem, and F. Ö. Ilday, *Opt. Lett.* **34**, 2516 (2009).